SANDIA REPORT SAND82—2534 • Unlimited Release • UC—60
Printed February 1984

FEB 23 1984

To	Org	Code
✓	1521	
✓	1522	
	1523	
	1524	
	1520	

1. Action 4. File
2. Info. 5. Destroy
3. See Me

A Comparison of Finite Element Predictions and Experimental Data for the Forced Response of the DOE 100 kW Vertical Axis Wind Turbine

Donald W. Lobitz, William N. Sullivan

Prepared by
Sandia National Laboratories
Albuquerque, New Mexico 87185 and Livermore, California 94550
for the United States Department of Energy
under Contract DE-AC04-76DP00789

Issued by Sandia National Laboratories, operated for the United States Department of Energy by Sandia Corporation.

NOTICE: This report was prepared as an account of work sponsored by an agency of the United States Government. Neither the United States Government nor any agency thereof, nor any of their employees, nor any of their contractors, subcontractors, or their employees, makes any warranty, express or implied, or assumes any legal liability or responsibility for the accuracy, completeness, or usefulness of any information, apparatus, product, or process disclosed, or represents that its use would not infringe privately owned rights. Reference herein to any specific commercial product, process, or service by trade name, trademark, manufacturer, or otherwise, does not necessarily constitute or imply its endorsement, recommendation, or favoring by the United States Government, any agency thereof or any of their contractors or subcontractors. The views and opinions expressed herein do not necessarily state or reflect those of the United States Government, any agency thereof or any of their contractors or subcontractors.

Printed in the United States of America
Available from
National Technical Information Service
U.S. Department of Commerce
5285 Port Royal Road
Springfield, VA 22161

NTIS price codes
Printed copy: A02
Microfiche copy: A01

TABLE OF CONTENTS

PAGE

Abstract 5

1. Introduction 5

2. Data Acquisition and Processing 6

3. Analysis Method and Finite Element Model 7

4. Results 9

4.1 Rotor Natural Frequencies 9

4.2 Centrifugal and Gravity Load Response 10

4.3 RMS Vibratory Stress Response 10

5. Concluding Remarks 14

Acknowledgements 14

References 15

A COMPARISON OF FINITE ELEMENT PREDICTIONS AND EXPERIMENTAL DATA FOR THE FORCED RESPONSE OF THE DOE 100kW VERTICAL AXIS WIND TURBINE*

D. W. Lobitz
W. N. Sullivan
Sandia National Laboratories
Albuquerque, New Mexico 87185

ABSTRACT

A specialized finite element capability has been developed to predict dynamic structural response of the vertical axis wind turbine (VAWT). This report is concerned with evaluating this finite element analysis technique. To achieve this, several types of experimental data taken from the DOE 100kW rotor are compared with predictions. These data include parked rotor natural frequencies, very low wind centrifugal and gravitational load response, and vibratory response from wind loads covering the rotor operational spectrum. Generally, the agreement between theory and experiment is very satisfactory. It is concluded that the analysis package is suitable for engineering design. Shortcomings observed in modeling accuracy are believed to be due primarily to inadequacies in blade aerodynamic load calculations.

1. INTRODUCTION

A part of the continuing DOE-sponsored research program on the vertical axis wind turbine (VAWT) has been concerned with the development of rotor structural modeling techniques. A variety of finite element based tools which have evolved from the DOE effort and others have been reported in the literature. These tools are intended to analyse several structural design issues, such as the determination of rotor modes and frequencies [1], identification of aeroelastic instabilities [2,3], and prediction of rotor response amplitudes due to aerodynamically applied loads [4]. Regarding the first two issues, relatively detailed efforts at experimental confirmation have been reported [1,2]. The third issue, response amplitudes for wind loading, is considerably more complex since it involves both structural dynamic modeling and aerodynamic load determination schemes. Because of this complexity and the limited availability of comprehensive structural data on operating rotors, there have been only qualitative attempts reported [4] to compare actual VAWT response data with predictions.

This report compares a particular rotor response analysis technique referred to as FFEVD [4] with experimental strain gage data collected from the DOE 100kW rotor [5]. FFEVD is a NASTRAN based finite element package which is still in a developmental stage. The version of FFEVD evaluated here includes advanced steady state (constant wind speed) streamtube-type aerodynamic models and previously identified important rotating system effects [8]. Not included in this investigation are damping effects (structural and aerodynamic) and unsteady loads due to atmospheric turbulence [9,10]. These effects may be important in some applications, but their inclusion in FFEVD requires additional theoretical work which is currently being developed.

Comparisons with the experimental data are made for two 100 KW rotor configurations. The tested configurations correspond to two guy cable support systems used which differ in axial cable stiffness by a factor of three. This change was effected to reduce rotor stresses by shifting a particular rotor mode frequency farther from a known excitation frequency [11].

Two aerodynamic models are used in FFEVD to establish sensitivity to load models. These models were CARDAA, a double-multiple

streamtube model with dynamic stall and variable Reynolds number effects [7], and FORCE, a simpler single streamtube device [6,12].

The 100kW rotor was instrumented with strain gages to experimentally evaluate the structural integrity of the rotor. Because of stress concentration effects, the gages as placed are not optimal for providing confirmation data for finite element models. Nonetheless, the instrumentation is sufficiently comprehensive to provide a useable data base. The strain gage data are processed on-site by minicomputer to a variety of reduction formats. The major format used here is the RMS vibratory strain level expressed as a function of the wind speed. This quantity is relatively easy to measure, is predictable by the analyses, and is itself an important factor for fatigue life estimation [13]. Other measures of rotor response, such as frequency spectra and mean stress levels, are also used in this report.

The following sections include a description of the experimental setup, discussion of the FFEVD package and the rotor finite element model, presentation of selected results, and concluding remarks.

2. DATA ACQUISITION AND PROCESSING

There are three nearly identical units of the DOE 100kW VAWT system in operation at Rocky Flats, Colo., Bushland, Tx., and Martha's Vineyard, Mass. All the data reported here came from the Bushland rotor since it is the most comprehensively instrumented.

Structural instrumentation referred to in this study consists of 18 strain gages located as shown in Figure 1a,b. Blade gages are concentrated at the four blade/tower connection regions (Fig. 1b). The blade/tower connection is effected with a "strongback" which is an extruded aluminum section welded to the blade to provide a flat surface for bolting the blade to the tower and strut attachment points. Gages to measure tower bending strains in and out of the rotor plane are located just below the mid-rotor flange. Experience with other VAWT rotors and the design analysis of the 100kW rotor [14] indicated that these locations experience the largest structural loads.

All the gages are set up for direct strain measurements and do not directly measure overall section loads. This is because the system was designed to assess component

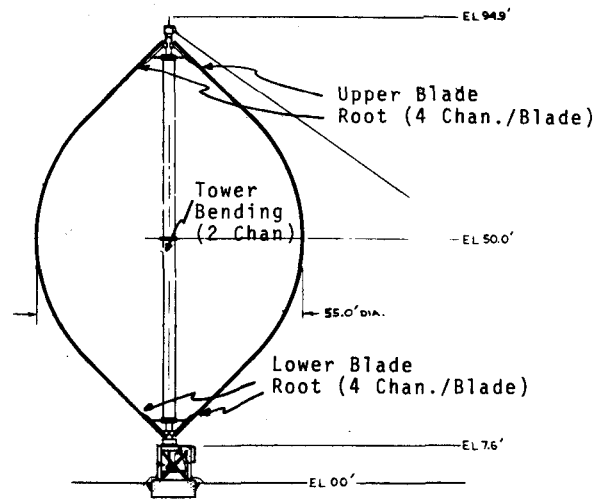

Figure 1a. Overall placement of strain gage instrumentation on the DOE 100kW rotor.

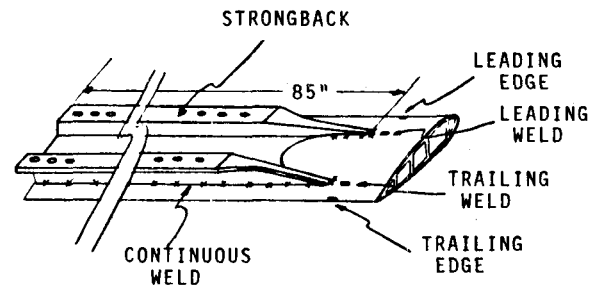

Figure 1b. Blade root gage detail. All root gages measure strain parallel to the long dimension of the blade.

integrity which is determined by strain. For finite element comparisons with data, overall section loads are more desirable. Unfortunately, load determination from direct strain readings is compromised somewhat by stress concentration factor uncertainties. This problem is most acute for the leading and trailing weld gages which are clearly in the vicinity of a stress riser. Laboratory measurements with test sections indicate that the stress concentration at the weld gages ranges from 1.1 to 1.5 for purely flatwise loading. The observed variability in stress concentration factors is evidently due to high strain gradients in the gage vicinity. This makes strain readings very sensitive to gage location and weld smoothness. To at least approximately account for the observed stress concentrations, the analytical

results for the weld gages are increased by a factor of 1.3. This correction is not used for the other rotor gages.

Analog outputs from the strain gage bridges are digitized to a ten bit binary word and serially multiplexed with a PCM (Pulsed Code Modulator) system attached to the rotor. The high level PCM output signal is passed to the data analysis software through a single pair of rotor sliprings. The sampling rate of the system corresponds to 100 readings/sec for each gage channel. All analog inputs to the PCM are low-pass filtered to 25hz to eliminate digital aliasing.

The PCM data are analysed on-site with a HP 1000 series minicomputer. Analysis software capabilities relevant to this report include the following:

(1) QUIK data analysis--All PCM channels are monitored for a five second period and the maximum, minimum and average values computed. These values are displayed on the console for all channels in a frequently updated tabular format.

(2) Strain BINS data--The "Method of Bins" [15] reduction scheme is used to determine the RMS strain vs. wind speed function for each strain gage channel. PCM data are monitored for one rotor revolution and the RMS and mean strain levels are computed along with the corresponding mean wind speed. The RMS level is defined as the root-mean-squared difference between strain readings over a revolution and the mean strain for that revolution. Histograms of strain RMS levels vs. wind speed "bins" may be created from thousands of rotor revolutions. By combining data taken on days with different wind conditions, the RMS strain levels can be determined for a wide range of wind speeds.

(3) Amplitude Spectra--Fast Fourier transform techniques are used to compute strain amplitude frequency spectra from stored time series data. The amplitude spectra are defined as the square root of the product of twice the spectral density and the bandwidth. In this report, the typical time series record length is 30 seconds. This yields a frequency resolution of .03 hz with a maximum frequency of 50hz.

Because of DC drift in strain gage bridge outputs, a process of zeroing the gages is required if absolute strain measurements are to be used. A state of zero strain is defined as a parked rotor in negligible winds. This definition allows relatively frequent zeroing of the gage system. The zeroing process does, however, eliminate gravitational loads from the measurements. This is inconsequential for vibratory strain measurements, but care must be used in interpreting mean strain levels.

3. ANALYSIS METHOD AND FINITE ELEMENT MODEL

The method of analysis is based on the finite element technique in order to provide modeling versatility. The development efforts have focused on the derivations of mass, damping and stiffness matrices, and force vectors appropriate for the VAWT. Due to the quasi-linear nature of the final VAWT equations of motion, existing solution procedures for static, eigenvalue and frequency response analysis can be used.

The equations of motion are developed relative to a coordinate system which rotates with the turbine at its angular velocity. Normally the use of a rotating frame results in the introduction of time-dependent coefficients because the support system (in this case the guy cables) does not rotate with the turbine. However, if the mass of the support system relative to the rotating components can be neglected, and its stiffness in the plane perpendicular to the axis of rotation approximated as isotropic, the support system can be modeled as though it were rotating with the turbine. For VAWTs these are reasonable approximations, and consequently, the total system can be modeled in the rotating frame without time-dependent coefficients. Rotating coordinate system effects, such as Coriolis and centrifugal forces, must still be included.

For small motions, u, relative to the rotating frame, the finite element equations of motion are represented by

$$[M]\{\ddot{u}\} + [C]\{\dot{u}\} - [S]\{u\} + [K]\{u\} = \{F_c\} + \{F_g\} + \{F_a\}. \qquad (1)$$

Here M and K are the mass and stiffness matrices. The quantities, C and S, which derive from rotating coordinate system effects, are the Coriolis and softening matrices respectively. The softening matrix

accounts for changes in the centrifugal force that result from the structural deformations. These last two matrices are developed in detail in [1].

On the right hand side of Equation (1), the three terms represent the centrifugal, gravitational and aerodynamic forces respectively. The first two are steady and do not change as the turbine rotates. The aerodynamic force, however, generally consists of steady and oscillatory components. For a steady wind, the oscillatory components are periodic with a period corresponding to one rotor revolution.

Solutions to Equation (1) would be routine except that a significant nonlinearity arises due to stretching of the blade in its long dimension. This stretching causes K to be a function of the deformation [16]. Inclusion of this nonlinearity in Equation (1) results in complex solution procedures. To avoid this, a revised stiffness matrix is developed commensurate with the quasi-static displacement field associated with the steady aerodynamic, centrifugal and gravitational loads only, neglecting the oscillatory components of the aerodynamic loads. This is accomplished through iterative solution of the following equation:

$$[K(u)]\{u\} = [S]\{u\}+\{F_c\}+\{F_g\}+\{\bar{F}_a\}, \qquad (2)$$

where $\bar{F}_a$ denotes the steady component of the aerodynamic loads. A revised stiffness matrix, K_r, obtained after iteration of Equation (2) is used in all subsequent calculations. Results from computations using K_r represent deformations about a state prestressed by gravitational, centrifugal, and steady aerodynamic loads.

In cases where the rotor is operated in very low winds, solutions of Equation (2) with $\{\bar{F}_a\}=\{0\}$ can be compared with experimental data. This is done in the next section under the subtitle of "Centrifugal and Gravity Load Response."

To obtain the modal characteristics of the rotor while rotating at a specified angular velocity, the right hand side of Equation (1) is set to zero. The stiffness matrix, however, corresponds to the prestressed state discussed above. The resulting Eigenvalue problem is Hermetian due to the skew-symmetry of the Coriolis matrix. Thus, in general the mode shapes will be complex and the natural frequencies are real. Complete development and validation of this procedure can be found in [1].

The frequency response of the rotor, driven by the oscillatory aerodynamic loads, is computed by solving the following variant of Equation (1) in the frequency domain:

$$[M]\{\ddot{u}\}+[C]\{\dot{u}\}-[S]\{u\}+[K_r]\{u\} = \{\tilde{F}_a\}. \qquad (3)$$

The vibratory aerodynamic forces, $\tilde{F}_a$, for steady wind conditions are computed using one of two aerodynamic load models. The more sophisticated of the two, CARDAA, is a double multiple streamtube model with wind shear, dynamic stall and variable Reynolds number effects [7]. The simpler one, FORCE, employs a single streamtube model [12]. In either case, the aerodynamic forces are computed for a reference blade as it turns through one complete revolution, taking care to represent the forces in the rotating coordinate system. These forces are then Fourier decomposed numerically in terms of "per rev" frequency components which represent integral multiples of the rotor angular rotational frequency, Ω, as shown below:

$$\begin{Bmatrix} F_x \\ F_y \\ F_z \end{Bmatrix}_r = \begin{Bmatrix} \sum A_{nx}\sin(n\Omega t) + B_{nx}\cos(n\Omega t) \\ \sum A_{ny}\sin(n\Omega t) + B_{ny}\cos(n\Omega t) \\ \sum A_{nz}\sin(n\Omega t) + B_{nz}\cos(n\Omega t) \end{Bmatrix} \qquad (4)$$

where the A_n's and B_n's are Fourier sine and cosine coefficients, respectively. The aerodynamic loads from either CARDAA or FORCE can be adequately represented with six Fourier harmonics.. Loads on other blades located azimuthally away from this reference blade by an angle, ϕ, are given by,

$$\begin{Bmatrix} F_x \\ F_y \\ F_z \end{Bmatrix}_\phi = \begin{Bmatrix} \cos\phi\ [\sum A_{nx}\sin(n\Omega t+n\phi)+B_{nx}\cos(n\Omega t+n\phi)] \\ -\sin\phi\ [\sum A_{ny}\sin(n\Omega t+n\phi)+B_{ny}\cos(n\Omega t+n\phi)] \\ \sin\phi\ [\sum A_{nx}\sin(n\Omega t+n\phi)+B_{nx}\cos(n\Omega t+n\phi)] \\ +\cos\phi\ [\sum A_{ny}\sin(n\Omega t+n\phi)+B_{ny}\cos(n\Omega t+n\phi)] \\ \sum A_{nz}\sin(n\Omega t+n\phi)+B_{nz}\cos(n\Omega t+\phi) \end{Bmatrix} \qquad (5)$$

In this manner the various per rev excitations are isolated and corresponding rotor responses are obtained with standard finite element frequency response solution procedures.

The frequency response results are in the form of sine and cosine response coefficients, C_n and D_n respectively, for each per rev excitation. To compare RMS vibratory test data with predictions, the RMS of the computed response is required.

The RMS is given in terms of the response coefficients by

$$\text{RMS} = \left[\sum (C_n^2 + D_n^2)/2\right]^{1/2} \qquad (6)$$

Because of its extensive library of solution procedures, the MacNeal-Schwendler version of NASTRAN [17] was selected for the implementation of the above analysis techniques. Procedures exist in NASTRAN for the iterative solution of Equation (2), complex eigenvalue analysis and complex frequency response computation. A minor amount of DMAP programming (a NASTRAN feature which allows the user to modify the code without dealing with the source code) is required to transfer the prestressed stiffness matrix to subsequent solution procedures.

For the frequency response computations, two special pre-processing tasks are performed in FFEVD. First, as there is no provision in NASTRAN for generating the Coriolis and softening matrices, they are developed in FFEVD and supplied to NASTRAN through its matrix input option. Secondly, aerodynamic loads for the blades are calculated, Fourier decomposed, and put in a form acceptable to NASTRAN. In both of these operations FFEVD reads the NASTRAN BULK DATA deck, extracts necessary information, performs the required computations, and adds the appropriate NASTRAN input cards to the BULK DATA deck. In this manner, the special considerations for the frequency response analysis of VAWTs are transparent to the user and the NASTRAN utilization appears relatively routine.

A special post-plotter has also been developed to help the user interpret the relatively large amount of NASTRAN output data.

Due to the simple structural nature of the VAWT, finite element models consist of beam elements (CBEAM elements in NASTRAN), concentrated masses and linear springs. The NASTRAN model of the DOE 100kW VAWT is shown in Figure 2.

Each blade is represented by 42 CBEAM elements, the tower is modeled by 12, and the blade struts by two each. The guy cables are accounted for by two orthogonal, horizontal springs attached at the top of the rotor, and a vertical load acting down through the tower. The torsional stiffness of the drive train is represented by a torsional spring, and concentrated masses are added at blade-to-blade joints and the mid-tower flange connection. The base of the rotor is considered to be infinitely stiff and is modeled by prohibiting translational motion at the thrust bearing.

Neither structural nor aerodynamic damping are included in this model.

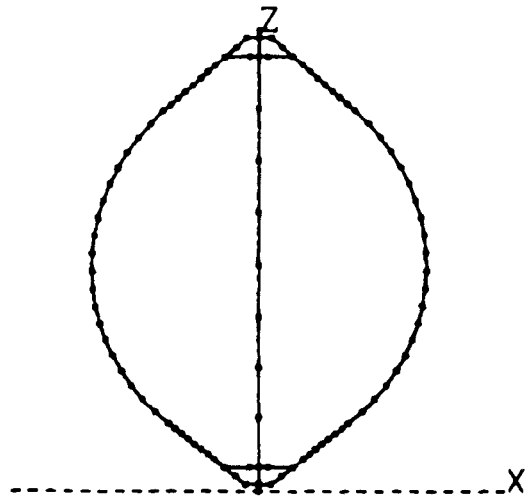

Fig. 2. NASTRAN finite element model of the DOE 100kW VAWT.

4. RESULTS

4.1 Rotor Natural Frequencies

A complete modal test was not conducted on the 100kW rotor. Partial measurements of the parked rotor modes were completed to aid in verifying the NASTRAN finite element model. Modal frequency data were obtained by monitoring free vibration response following hand excitation of the rotor using personnel suspended from a crane. By pushing the rotor by hand in the appropriate direction and frequency at a soft point of the rotor, it is possible for an individual to selectively excite the lowest frequency modes to amplitudes measurable by the strain gages. This technique was used to determine the frequencies of the first five rotor modes.

Table 1 summarizes a comparison between the measured free vibration modes and those predicted by the NASTRAN finite element model. The agreement between measurements and NASTRAN is excellent. This confirms that the finite element model is a good dynamic representation of the physical structure.

Table 1. Parked Rotor Natural Frequencies

Mode # and Description	Freq.(hz) Meas.	Freq.(hz) Theory
1. first flatwise, blade "drooping"	1.7	1.6-1.6*
2. first "butterfly" rotor out-of-plane	2.2	2.1
3. first tower bending in-plane	2.7	2.7
4. 2nd "butterfly" out-of-plane	3.4	3.5
5. 2nd flatwise blade	3.6	3.6-3.7*

* Double modes corresponding to symmetric and antisymmetric rotor responses.

Table 2. Centrifugal and Gravitational Blade Stresses, 48.1 RPM Rotor Speed

Gage: (Fig.1b)	Leading Edge	Leading Weld	Trailing Weld	Trailing Edge
Theory, upper root	1236	-1166	-84	1236
Meas., upper root	1375	210	423	n.a.
Theory, lower root	1238	-6445	-4117	1238
Meas., lower root	1756	-4057	-3857	1507

Notes: units for stress are psi; positive stresses are tensile; all results shown are less gravity-only stresses (see text).

4.2 Centrifugal and Gravity Load Response

Purely centrifugal and gravitational loads may be applied to the rotor simply by motoring the turbine in negligible winds. This load system is well defined and the results are helpful in locating errors in the finite element model or the instrumentation system.

Finite element analysis of this test is a statics problem since all the applied loads are steady. The analysis is effected as described in Section 3. Initially, the response due to both centrifugal and gravity loads is calculated. Response from another calculation for gravity loading only is then subtracted from the centrifugal and gravitational load results. This is done since the measured data has gravity loading effectively subtracted due to the gage zeroing process. This process is not quite equivalent to analyzing or testing with only centrifugal loads. This is because the rotor stiffness generally changes for the different load cases and thus linear load superposition is not applicable.

Table 2 shows predicted and measured stress levels for all the blade gage locations of Figure 1. The agreement is fair for the leading and trailing edge gages and poor for the weld gages. It is believed that the lack of agreement for this well defined test is primarily due to complex stress concentration effects near the blade root. This test involves both blade axial and flatwise bending loads. This precludes assigning a single stress concentration factor to the analysis. Although limited data were obtained on flatwise bending stress concentrations (see Data Acquisition section, above), none are available for axial loading. Since the axial load path from the blade to the tower passes exclusively through the strongback welds, it is likely there are high axial load stress concentrations near the weld terminations. The fact that the weld strain gage measurements in Table 2 are more tensile than predictions is consistent with this hypothesis.

Although the stress concentration issue prevents this test from solidly verifying the finite element static analysis, it is apparent that the model reasonably predicts rotor response to static loads.

4.3 RMS Vibratory Stress Response

RMS vibratory stress data are available for the DOE 100kW VAWT in two structural configurations. The difference consists of a three to one ratio in the guy cable stiffness, and hereafter the two designs will be identified as either the soft or stiff cable configuration. As the soft cable data was taken during the heat of the summer in Bushland, Tx., the aerodynamic loads for the frequency response analyses were computed with an air density of .066 lbm/ft3. On the other hand, the stiff cable data was taken during the winter with a corresponding density of .072 lbm/ft3. In all cases where the CARDAA aerodynamic model was used, the wind shear factor was set at .17, a reasonable value for the site. For the weld gage locations, the predictions

were multiplied by a factor of 1.3 to account for the stress concentration which exists in the hardware but not in the NASTRAN model. This value was obtained from laboratory measurements done on the section in question.

Both aerodynamic models were used in the predictions, and, in general, the FORCE model substantially underpredicts the data, whereas the CARDAA model demonstrates much better agreement. Consequently, since CARDAA is considered to be the most accurate of the two models, the majority of the predictions are made using it, and only a few with FORCE in order to demonstrate the differences.

The level of agreement between data and predictions was similar for the two turbine configurations. Thus, to avoid repetition, only a few comparisons for the soft cable configuration are included here.

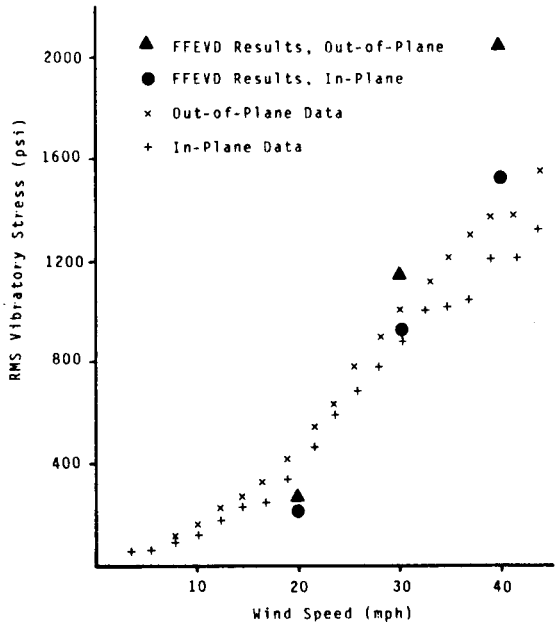

Fig. 3. RMS vibratory rotor tower stresses for the stiff cable configuration, CARDAA aerodynamic model.

Figure 3 shows RMS vibratory stress comparisons between predictions and data for the rotor tower in the stiff cable configuration, using the CARDAA aerodynamic model. The theory tends to underpredict in low winds and overpredict in high ones. The observation that the out-of-plane response is greater than the in-plane is correctly predicted.

Comparisons for the blade edgewise response are shown in Figure 4. In this figure and subsequent ones, the x's represent data for one of the blades, and the +'s, the other.

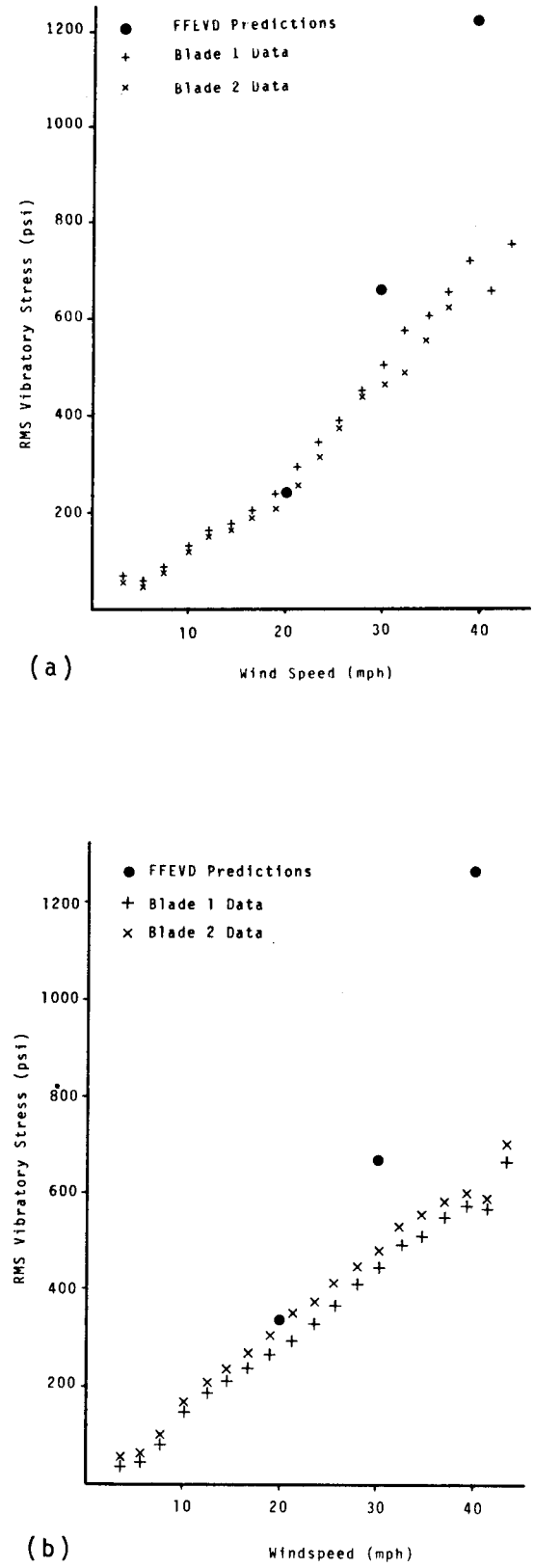

Fig. 4. RMS vibratory blade edgewise stresses for the stiff cable configuration, CARDAA aerodynamic model: (a) lower trailing edge, (b) upper leading edge.

These two sets provide a measure of the repeatability of the data. As with the tower comparisons, the theory overpredicts response in high winds. However, at low wind speeds the agreement is quite good.

The blade weld gage comparisons are shown in Figure 5. Generally the agreement between the predictions and the data is very satisfactory. However, referring to parts a and b of Figure 5, the inconsistency in the corresponding data from each blade produces some uncertainty in assessing the level of agreement for this case.

RMS vibratory stress comparisons for the soft cable configuration are shown in Figures 6, 7 and 8. Using the CARDAA aerodynamic model, the agreement between data and predictions is similar to that obtained for the stiff cable configuration. On these curves several points are included which correspond to predictions using the FORCE aerodynamic model. These points tend to severely underpredict the data in low winds, with better agreement for the higher wind speeds. In general, however, the FORCE results are inferior to and less conservative than those made with CARDAA.

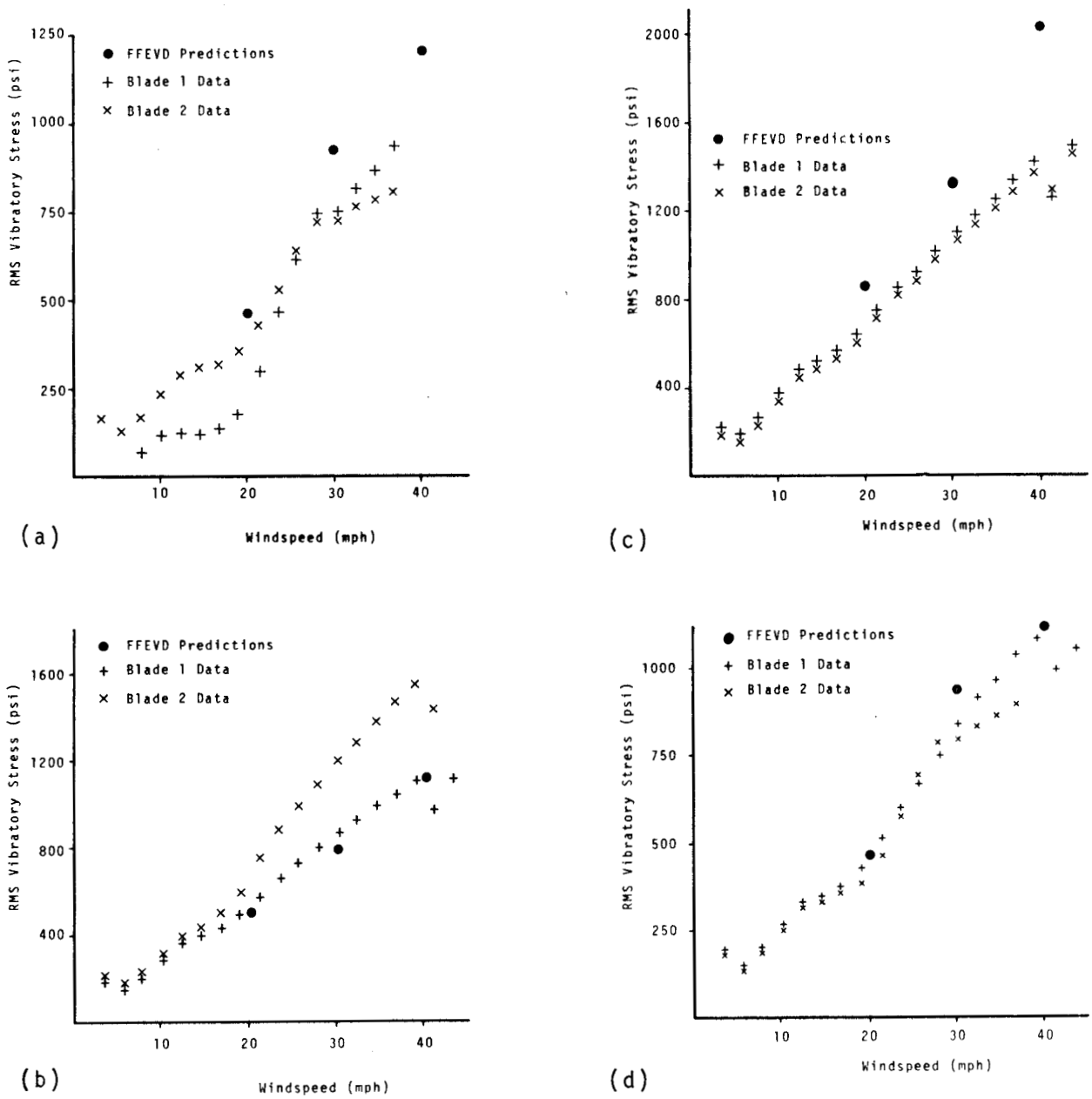

Fig. 5. RMS vibratory blade flatwise stresses for the stiff cable configuration, CARDAA aerodynamic model; (a) upper trailing weld, (b) lower trailing weld, (c) upper leading weld, (d) lower leading weld.

Contrasting the corresponding curves for the soft and stiff cable configurations, the change to stiff cables has significantly reduced the edgewise blade response (Figures 4a and 7), especially when a 10% increase is applied to the soft cable data to normalize it to the winter air density. Applying this same factor to the flatwise soft cable data, the flatwise response has also decreased, although less dramatically (Figures 5d and 8). Alternatively, the the tower response has increased (Figures 3 and 6) and the

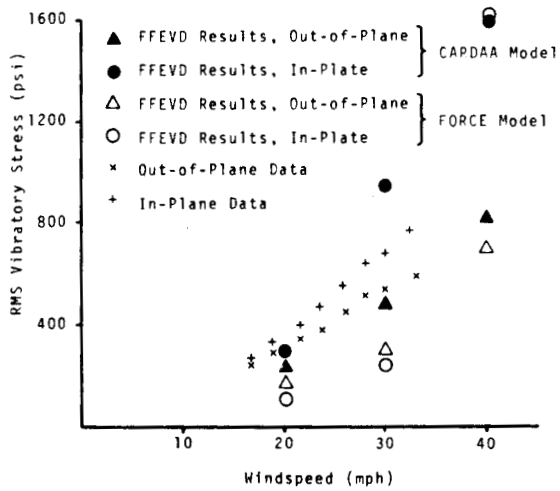

Fig. 6. RMS vibratory rotor tower stresses for the soft cable configuration.

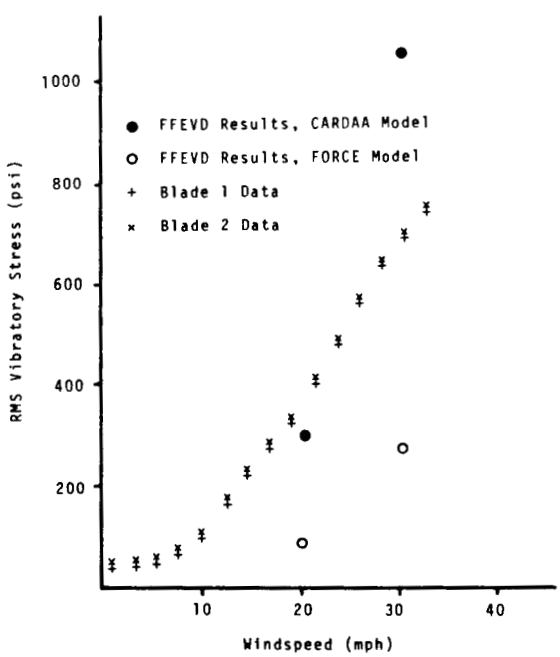

Fig. 7. RMS vibratory blade edgewise stresses for the soft cable configuration, lower trailing edge.

dominant response has shifted from in-plane to out-of-plane for the stiffer cables. This shift is correctly predicted by the finite element model. Both the test data and the analysis predictions confirm that the stress reductions sought by the installation of stiff cables were achieved.

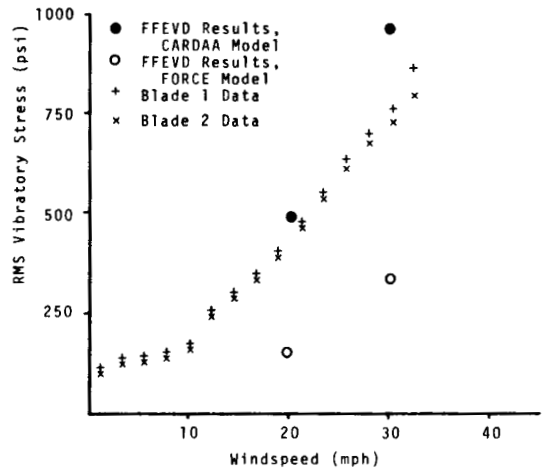

Fig. 8. RMS vibratory blade flatwise stresses for the soft cable configuration, lower leading weld.

For both cable configurations, the analytical results for the tower and edgewise blade response generally overpredict the data for high winds. There are several possible explanations for this

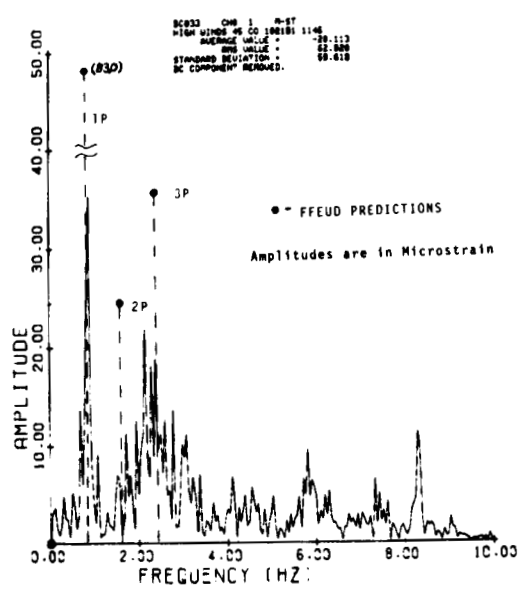

Figure 9(a). Amplitude spectrum for upper leading edge gage, 30mph winds.

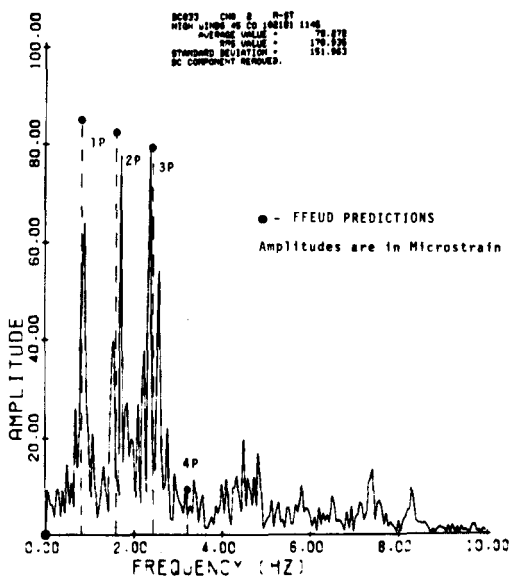

Figure 9(b). Amplitude spectrum for upper leading weld gage, 30mph winds.

disagreement. One major difficulty with the analysis is seen from examining amplitude spectra of gage response. Two such spectra are shown in Figure 9 for the leading edge and leading weld gages, respectively. Note that the theory predicts response only at the integral per revs of the rotor speed as discussed in Section 3. It is apparent from Figure 9 that the rotor experiences a more broad-banded response. This is believed to be due to atmospheric turbulence. Either because of turbulence or basic inaccuracies in the aerodynamic load model, the 1 per rev response component is considerably overpredicted for the leading edge gage. Another factor is that the method of bins data analysis technique tends to underestimate the response near the high wind end where the data are relatively sparse [15]. The effects of both structural and aerodynamic damping, neither of which have been included in the analysis, may also reduce the predictions.

5. CONCLUDING REMARKS

All the results presented indicate that the FFEVD analysis package is a very useful engineering design tool. The analysis produced credible predictions of all the structural data obtained for two configurations of the 100kW rotor operated over a wide range of wind speeds.

While the level of agreement is encouraging, FFEVD clearly does not absolutely predict all response details with high accuracy. This is undoubtedly due to the simplifying assumptions currently imbedded in the theory and to experimental difficulties. It is worthwhile to consider where the likely sources of error are in this study and to discuss ways to eliminate or reduce them:

(1) Aerodynamic Load Modeling--Any linear forced vibration analysis produces responses which are proportional to the applied loads. The differences in results produced by the CARDAA and FORCE load models demonstrates this. While CARDAA represents the state-of-the-art in streamtube modeling approaches, it has only been partially verified by comparing predicted and measured average rotor shaft torque. Furthermore, both the CARDAA and FORCE models are based on steady winds with the consequence that forces are produced exclusively at discrete frequencies related to the rotor speed. Examination of the response spectra clearly show that atmospheric turbulence spoils such a simple representation of load spectra. Efforts are in progress to model unsteady load effects [9] and to directly measure aerodynamic forces on VAWT blades [18]. These efforts should lead to improved load models for future application in FFEVD.

(2) Experimental Technique--The gaging of the 100kW rotor was not arranged best for obtaining confirmation data. It is recommended on future tests that blade gaging be arranged to measure tension, flatwise moments, and edgewise moments rather than direct strain. This can be done by locating active bridge elements far from stress concentrations and by calibrating the bridges with known loads prior to blade installation

(3) Rotor Damping-- The structural damping of typical VAWT rotors is very low (the order of 1% of critical [19]). Inclusion of damping of this magnitude will have a negligible effect on FFEVD results for non-resonant operations. However, aerodynamic damping can, for certain rotor modes, approach 5% of critical [2,3]. This may be large enough to influence non-resonant results. Inclusion of aerodynamic damping into FFEVD is complex but can be done without altering the basic structure of the package.

ACKNOWLEDGEMENTS

The information in this report was obtained with the valuable support of many individuals involved with the DOE VAWT research program. The 100kW rotor instrumentation system was designed and

implemented by J. Burkhardt. R. N. Clark and R. Davis of USDA provided valuable assistance in the day-to-day maintenance of the instrumentation system and the rotor itself. The RMS strain bins data analysis program was designed and implemented by P. S. Veers and J. McNerney. FFEVD pre- and post-processors were developed by T. M. Leonard with contributions from R. A. Watson. D. J. Malcolm of DAF Indal (Canada) made corrections which directly resolved technical difficulties with the early versions of FFEVD. Finally, D. E. Berg and T. M. Leonard prepared and debugged the CARDAA load subroutines used in FFEVD.

REFERENCES

[1] Carne,T.G., Lobitz,D.W., Nord,A.R., and Watson,R.A., "Finite Element Analysis and Modal Testing of a Rotating Wind Turbine," Sandia Report SAND82-0345, October 1982.

[2] Popelka,D., "Aeroelastic Stability of a Darrieus Wind Turbine," Sandia Report SAND82-0672, March 1982.

[3] Vollan,A.J.,and Zwaan,R.J., "Contribution of NLR to the first Phase of the National Research Program on Wind Energy, Part I: Elastomechanical and Aeroelastic Stability," National Aerospace Laboratory NLR, The Netherlands, Report NLR TR 78072 L June 1978.

[4] Lobitz,D.W., "Forced Vibration Analysis of Rotating Structures with Application to Vertical Axis Wind Turbines," Proceedings (Vol III), Fifth Biennial Wind Energy Conference and Workshop, Oct. 1981, SERI/CP-635-1340.

[5] Nellums,R.O., "Status Report on the 17-m VAWT Program," Proceedings (Vol I), Fifth Biennial Wind Energy Conference and Workshop, Oct. 1981, SERI/CP-635-1340.

[6] Templin,R.J., "Aerodynamic Performance Theory for the NRC Vertical Axis Wind Turbine," NRC Report LTR-LA- 160, June 1974.

[7] Paraschivoiu,I., "Aerodynamic Loads and Performance of the Darrieus Rotor," AIAA J. of Energy, Vol 6 No 6, pp 406-412, Dec. 1982

[8] Sullivan,W.N., "Structural Dynamic Response Characteristics of Darrieus Vertical Axis Wind Turbines," Proceedings (Vol I), Fifth Biennial Wind Energy Conference and Workshop, Oct. 1981, SERI/CP-636-1340

[9] Veers,P.S., "Aerodynamic Considerations for Stochastic Loading," presentation at the Third Annual SNL VAWT Aerodynamic Seminar, Mar. 24-25, 1983, Sandia National Labs, Albuquerque, N. M.

[10] Akins,R.E., "Rotationally-Sampled Flow Field Measurements for Vertical Axis Wind Turbines," presented at Univ. of Missouri-Columbia Wind/Solar Energy Technology Conference, Kansas City, Mo., April 25-26, 1983.

[11] Carne,T.G., "Guy Cable Design and Damping for Vertical Axis Wind Turbines," Proceedings, Wind Turbine Dynamics Workshop, Cleveland, Oh., Feb. 1981, DOE publication CONF-810226.

[12] Sullivan,W.N., and Leonard,T.M., "A Computer Subroutine for Estimating Aerodynamic Blade Loads on Darrieus Vertical Axis Wind Turbines," Sandia Report SAND80-2407, Nov., 1980.

[13] Veers,P.S., "Blade Fatigue Life Assessment with Application to VAWTs," Proceedings (Vol II), Fifth Biennial Wind Energy Conference and Workshop, Oct. 1981, SERI/CP-636-1340.

[14] Sullivan,W.N., "Static Blade Analysis of the DOE/Alcoa Low Cost 17 Meter Turbine," Proceedings of the VAWT Design Technology Seminar for Industry, Sandia Report SAND80-0984, April, 1980.

[15] Akins,R.E., "Method of Bins Update," Proceedings for AWEA Wind Energy Expo '82, Amarillo, Tx, Oct. 24-27, 1982.

[16] Weingarten,L.I., and Nickell,R.E., "Non-Linear Stress Analysis of Vertical Axis Turbine Blades," Sandia Report SAND74-0378, April 1975.

[17] MSC/NASTRAN User's Manual, Vols I and II, The MacNeal-Schwendler Corp., 1981.

[18] Akins,R.E., Climas,P.C., and Croll,R. H., "Pressure Distributions on an Operating VAWT Blade Element," Proceedings, ASES Wind Workshop VI, June 1-3, Minneapolis, Minn.(to be published)

[19] Carne,T.G., and Nord,A.R., "Modal Testing of a Rotating Wind Turbine", Sandia Report SAND82-0631, Nov. 1981.

DISTRIBUTION:

Aerolite, Inc.
550 Russells Mills Road
South Dartmouth, MA 02748
Attn: R. K. St. Aubin

Alcoa Technical Center (4)
Aluminum Company of America
Alcoa Center, PA 15069
Attn: D. K. Ai
J. T. Huang
J. R. Jombock
J. L. Prohaska

Alternative Sources of Energy
Milaca, MN 56353
Attn: Larry Stoiaken

Amarillo College
Amarillo, TX 79100
Attn: E. Gilmore

American Wind Energy Association
1516 King Street
Alexandria, VA 22314

Arizona State University
University Library
Tempe, AZ 85281
Attn: M. E. Beecher

Atlantic Wind Test Site
P.O. Box 189
Tignish P.E.I.
CANADA COB 2BO
Attn: R. G. Richards

Battelle-Pacific Northwest Laboratory
P.O. Box 999
Richland, WA 99352
Attn: Larry Wendell

Dr. George Bergeles
Dept. of Mechanical Engineering
National Technical University
42, Patission Street
Athens, GREECE

Bonneville Power Administration
P.O. Box 3621
Portland, OR 97225
Attn: N. Butler

Burns & Roe, Inc.
800 Kinderkamack Road
Oradell, NJ 07649
Attn: G. A. Fontana

California State Energy Commission
Research and Development Division
1111 Howe Avenue
Sacramento, CA 95825
Attn: J. Lerner

Canadian Standards Association
178 Rexdale Blvd.
Rexdale, Ontario
CANADA M9W 1R3
Attn: Tom Watson

Professor V. A. L. Chasteau
School of Engineering
University of Auckland
Private Bag
Auckland, NEW ZEALAND

Colorado State University
Dept. of Civil Engineering
Fort Collins, CO 80521
Attn: R. N. Meroney

Commonwealth Electric Co.
Box 368
Vineyard Haven, MA 02568
Attn: D. W. Dunham

Cornell University
Dept. of Mechanical and Aerospace Engineering
Upson Hall
Ithaca, NY 14853
Attn: Gary Wayne

Gale B. Curtis
Curtis Associates
3089 Oro Blanco Drive
Colorado Springs, CO 80917

M. M. Curvin
11169 Loop Road
Soddy Daisy, TN 37379

Department of Economic Planning
and Development
Barrett Building
Cheyenne, WY 82002
Attn: G. N. Monsson

Otto de Vries
National Aerospace Laboratory
Anthony Fokkerweg 2
Amsterdam 1017
THE NETHERLANDS

DOE/ALO
Albuquerque, NM 87115
Attn: G. P. Tennyson

DOE/ALO
Energy Technology Liaison Office
NGD
Albuquerque, NM 87115
Attn: Capt. J. L. Hanson, USAF

DOE Headquarters (20)
Wind Energy Technology Division
1000 Independence Avenue
Washington, DC 20585
Attn: L. V. Divone
P. Goldman

Dominion Aluminum Fabricating, Ltd. (2)
3570 Hawkestone Road
Mississauga, Ontario
CANADA L5C 2V8
Attn: L. Schienbein
C. Wood

J. B. Dragt
Nederlands Energy Research Foundation (E.C.N.)
Physics Department
Westerduinweg 3 Patten (nh)
THE NETHERLANDS

Dynergy Systems Corporation
821 West L Street
Los Banos, CA 93635
Attn: C. Fagundes

Dr. Norman E. Farb
10705 Providence Drive
Villa Park, CA 92667

Electric Power Research Institute (3)
3412 Hillview Avenue
Palo Alto, CA 94304
Attn: E. Demeo
F. Goodman
S. Kohan

Alcir de Faro Orlando
Pontificia Universidade Catolica-PUC/Rj
Mechanical Engineering Department
R. Marques de S. Vicente 225
Rio de Janeiro, BRAZIL

FloWind Corporation (4)
21414 68th Avenue South
Kent, WA 98031
Attn: Herman M. Drees
S. Tremoulet
I. E. Vas
R. Watson

Gates Learjet
Mid-Continent Airport
P.O. Box 7707
Wichita, KS 67277
Attn: G. D. Park

H. Gerardin
Mechanical Engineering Department
Faculty of Sciences and Engineering
Universite Laval-Quebec
CANADA G1K 7P4

R. T. Griffiths
University College of Swansea
Dept. of Mechanical Engineering
Singleton Park
Swansea SA2 8PP
UNITED KINGDOM

Helion, Inc.
Box 445
Brownsville, CA 95919
Attn: Jack Park, President

Institut de recherche d'Hydro-Quebec (3)
1800, Montee Ste-Julie
Varennes, Quebec
Canada JOL 2PO
Attn: Gaston Beaulieu
Bernard Masse
Ion Paraschivoiu

Iowa State University
Agricultural Engineering, Room 213
Ames, IA 50010
Attn: L. H. Soderholm

JBF Scientifcic Corporation
2 Jewel Drive
Wilmington, MA 01887
Attn: E. E. Johanson

Kaiser Aluminum and Chemical Sales, Inc.
14200 Cottage Grove Avenue
Dolton, IL 60419
Attn: A. A. Hagman

Kaiser Aluminum and Chemical Sales, Inc.
6177 Sunol Blvd.
P.O. Box 877
Pleasonton, CA 94566
Attn: D. D. Doerr

Kaman Aerospace Corporation
Old Windsor Road
Bloomfield, CT 06002
Attn: W. Batesol

Kansas State University
Electrical Engineering Department
Manhattan, KS 66506
Attn: Dr. G. L. Johnson

R. E. Kelland
The College of Trades and Technology
P.O. Box 1693
Prince Philip Drive
St. John's, Newfoundland
CANADA A1C 5P7

KW Control Systems, Inc.
RD#4, Box 914C
South Plank Road
Middletown, NY 10940
Attn: R. H. Klein

Kalman Nagy Lehoczky
Cort Adelers GT. 30
Oslo 2
NORWAY

L. Liljidahl
Building 005, Room 304
Barc-West
Beltsville, MD 20705

Olle Ljungstrom
FFA, The Aeronautical Research Institute
Box 11021
S-16111 Bromma
SWEDEN

Massachusetts Institute of Technology (2)
77 Massachusetts Avenue
Cambridge, MA 02139
Attn: Professor N. D. Ham
W. L. Harris, Aero/Astro Dept.

H. S. Matsuda
Composite Materials Laboratory
Pioneering R&D Laboratories
Toray Industries, Inc.
Sonoyama, Otsu, Shiga
JAPAN 520

Michigan State University
Division of Engineering Research
East Lansing, MI 48825
Attn: O. Krauss

The Mitre Corporation
1820 Dolley Madison Blvd.
McLean, VA 22102
Attn: F. R. Eldridge, Jr.

Napier College of Commerce and Technology
Tutor Librarian, Technology Faculty
Colinton Road
Edinburgh, EH10 5DT
ENGLAND

NASA Lewis Research Center (2)
21000 Brookpark Road
Cleveland, OH 44135
Attn: D. Baldwin
J. Savino

National Rural Electric Cooperative Assn
1800 Massachusetts Avenue NW
Washington, DC 20036
Attn: Wilson Prichett III

Natural Power, Inc.
New Boston, NH 03070
Attn: Leander Nichols

Northwestern University
Dept. of Civil Engineering
Evanston, IL 60201
Attn: R. A. Parmalee

Ohio State University
Aeronautical and Astronautical Dept.
2070 Neil Avenue
Columbus, OH 43210
Attn: Professor G. Gregorek

Oklahoma State University
Mechanical Engineering Dept.
Stillwater, OK 76074
Attn: D. K. McLaughlin

Oregon State University (2)
Mechanical Engineering Dept.
Corvallis, OR 97331
Attn: R. W. Thresher
R. E. Wilson

Pacific Gas & Electric
3400 Crow Canyon Road
San Ramon, CA 94583
Attn: T. Hillesland

Troels Friis Pedersen
Riso National Laboratory
Postbox 49
DK-4000 Roskilde
DENMARK

Helge Petersen
Riso National Laboratory
DK-4000 Roskilde
DENMARK

The Power Company, Inc.
P.O. Box 221
Genesee Depot, WI 53217
Attn: A. A. Nedd

Public Service Co. of New Hampshire
1000 Elm Street
Manchester, NH 03105
Attn: D. L. C. Frederick

Public Service Company of New Mexico
P.O. Box 2267
Albuquerque, NM 87103
Attn: M. Lechner

RANN, Inc.
260 Sheridan Ave., Suite 414
Palo Alto, CA 94306
Attn:Alfred J. Eggers, Jr.
Chairman of the Board

Renewable Energy Ventures
190 South King Street, Suite 2460
Honolulu, HI 96813
Attn: G. W. Stricker

The Resources Agency
Department of Water Resources
Energy Division
1416 9th Street
P.O. Box 388
Sacramento, CA 95802
Attn: R. G. Ferreira

Reynolds Metals Company
Mill Products Division
6601 West Broad Street
Richmond, VA 23261
Attn: G. E. Lennox

A. Robb
Memorial University of Newfoundland
Faculty of Engineering and Applied Sciences
St. John's Newfoundland
CANADA A1C 5S7

Rockwell International (2)
Rocky Flats Plant
P.O. Box 464
Golden, CO 80401
Attn: Terry Healy

Dr. -Ing. Hans Ruscheweyh
Institut fur Leichbau
Technische Hochschule Aachen
Wullnerstrasse 7
GERMANY

Beatrice de Saint Louvent
Establissement d'Etudes et de Recherches
Meteorologigues
77, Rue de Serves
92106 Boulogne-Billancourt Cedex
FRANCE

Gwen Schreiner
Librarian
National Atomic Museum
Albuquerque, NM 87185

Arnan Seginer
Professor of Aerodynamics
Technion-Israel Institute of Technology
Department of Aeronautical Engineering
Haifa, ISRAEL

David Sharpe
Kingston Polytecnic
Canbury Park Road
Kingston, Surrey
UNITED KINGDOM

Kent Smith
Instituto Technologico Costa Rico
Apartado 159 Cartago
COSTA RICA

Solar Initiative
Citicorp Plaza, Suite 900
180 Grand Avenue
Oakland, CA 94612
Attn: Jerry Yudelson

Bent Sorenson
Roskilde University Center
Energy Group, Bldg. 17.2
IMFUFA
P.O. Box 260
DK-400 Roskilde
DENMARK

South Dakota School of Mines and Technology
Dept. of Mechanical Engineering
Rapid City, SD 57701
Attn: E. E. Anderson

Southern California Edison
Research & Development Dept., Room 497
P.O. Box 800
Rosemead, CA 91770
Attn: R. L. Scheffler

Southern Illinois University
School of Engineering
Carbondale, IL 62901
Attn: C. W. Dodd

G. Stacey
The University of Reading
Department of Engineering
Whiteknights, Reading, RG6 2AY
ENGLAND

Stanford University
Dept. of Aeronautics and
Astronautics Mechanical Engineering
Stanford, CA 94305
Attn: Holt Ashley

R. J. Templin (3)
Low Speed Aerodynamics Laboratory
NRC-National Aeronautical Establishment
Montreal Road
Ottawa, Ontario
CANADA K1A OR6

Texas Tech University (2)
Mechanical Engineering Dept.
P.O. Box 4389
Lubbock, TX 79409
Attn: J. W. Oler
J. Strickland

Tulane University
Dept. of Mechanical Engineering
New Orleans, LA 70018
Attn: R. G. Watts

Tumac Industries, Inc.
650 Ford Street
Colorado Springs, CO 80915
Attn: J. R. McConnell

J. M. Turner
Terrestrial Energy Technology Program Office
Energy Conversion Branch
Aerospace Power Division
Aero Propulsion Laboratory
Air Force Wright Aeronautical Laboratories (A
Wright-Patterson Air Force Base, OH 45433

United Engineers and Constructors, Inc.
PO Box 8223
Philadelphia, PA 19101
Attn: A. J. Karalis

University of Alaska
Geophysical Institute
Fairbanks, AK 99701
Attn: T. Wentink, Jr.

University of California
Institute of Geophysics
and Planetary Physics
Riverside, CA 92521
Attn: Dr. P. J. Baum

University of Colorado
Dept. of Aerospace Engineering Sciences
Boulder, CO 80309
Attn: J. D. Fock, Jr.

University of Massachusetts
Mechanical and Aerospace Engineering Dept.
Amherst, MA 01003
Attn: Dr. D. E. Cromack

University of New Mexico
New Mexico Engineering Research Institute
Campus P.O. Box 25
Albuquerque, NM 87131
Attn: G. G. Leigh

University of Oklahoma
Aero Engineering Department
Norman, OK 73069
Attn: K. Bergey

University of Sherbrooke
Faculty of Applied Science
Sherbrooke, Quebec
CANADA J1K 2R1
Attn: R. Camerero

The University of Tennessee
Dept. of Electrical Engineering
Knoxville, TN 37916
Attn: T. W. Reddoch

USDA, Agricultural Research Service
Southwest Great Plains Research Center
Bushland, TX 79012
Attn: Dr. R. N. Clark

Utah Power and Light Co.
51 East Main Street
P.O. Box 277
American Fork, UT 84003
Attn: K. R. Rasmussen

VAWTPOWER, Inc.
9733 Coors NW
Albuquerque, NM 87114
Attn: P. N. Vosburgh

Washington State University
Dept. of Electrical Engineering
Pullman, WA 99163
Attn: F. K. Bechtel

West Texas State University
Government Depository Library
Number 613
Canyon, TX 79015

West Texas State University
Department of Physics
P.O. Box 248
Canyon, TX 79016
Attn: V. Nelson

West Virginia University
Dept. of Aero Engineering
1062 Kountz Avenue
Morgantown, WV 26505
Attn: R. Walters

D. Westlind
Central Lincoln People's Utility District
2129 North Coast Highway
Newport, OR 97365-1795

Wichita State University
Aero Engineering Department (2)
Wichita, KS 67208
Attn: M. Snyder
W. Wentz

Wind Energy Report
Box 14
102 S. Village Avenue
Rockville Centre, NY 11571
Attn: Farrell Smith Seiler

Wind Power Digest
P. O. Box 700
Bascom, OH 44809
Attn: Michael Evans

Wisconsin Division of State Energy
8th Floor
101 South Webster Street
Madison, WI 53702
Attn: Wind Program Manager

1520	D. J. McCloskey
1522	R. C. Reuter, Jr.
1523	D. B. Clauss
1524	D. W. Lobitz (5)
1524	P. S. Veers
1524	W. N. Sullivan (5)
1630	R. C. Maydew
1633	R. E. Sheldahl
1636	J. K. Cole
1636	D. E. Berg
2525	R. P. Clark
3141	L. J. Erickson (5)
3151	W. L. Garner (3)
3154-3	C. H. Dalin (25) For DOE/TIC (Unlimited Release)
3160	J. E. Mitchell (15)
3161	P. S. Wilson
6000	E. H. Beckner
6200	V. L. Dugan
6220	D. G. Schueler
6225	R. H. Braasch (50)
6225	J. D. Cyrus
6225	R. D. Grover
6225	E. G. Kadlec
6225	P. C. Klimas
6225	M. T. Mattison
6225	R. O. Nellums
6225	D. S. Oscar
6225	M. H. Worstell
7111	J. W. Reed
8214	M. A. Pound